

Modelling and Influences of Transmitter and Receiver Nonlinearities in Optical OFDM Transmission

Henning Paul and Karl-Dirk Kammeyer
 Department of Communications Engineering
 University of Bremen, 28359 Bremen, Germany
 Email: {paul, kammeyer}@ant.uni-bremen.de

Abstract—In this paper, the main sources of nonlinear distortions for back-to-back (B2B) transmission in an Intensity Modulation/Direct Detection (IM/DD) fiber optical system are presented. The nonlinear characteristics are modelled and their impact on an OFDM signal are described by means of stochastic considerations. Furthermore, the dependence of nonlinear distortions on tunable key parameters of the optical transmission system is analyzed. Its performance depending on these parameters is evaluated by means of computer simulations.

Index Terms—Optical OFDM, Nonlinearities, B2B, IM/DD

I. INTRODUCTION

ORTHOGONAL Frequency Division Multiplexing (OFDM) is a promising new approach for the optical long-haul high-speed data transmission over single-mode fibers due to the ease of channel equalization. In fiber optical communications, the channel usually has an all-pass characteristic with a phase response governed by group velocity dispersion resulting from the optical fiber [1]. However, the nonlinearities introduced by modulator and detector components of the optical system, but also the nonlinearities introduced by the fiber itself pose a challenge to OFDM. Thus, the impact of these nonlinear effects has to be analyzed.

In this paper, we will restrict to the nonlinearities of modulator and detector for the sake of simplicity, thus only the so-called back-to-back (B2B) case with no fiber involved will be considered. The optical fiber itself would cause the memoryless nonlinearities considered here to turn into a nonlinearity with memory which has to be analyzed in future works.

This work was supported by the German Research Foundation (DFG) under grant Ka814/19.

II. SYSTEM MODEL

The Zero-IF (Intermediate Frequency) Intensity Modulation/Direct Detection (IM/DD) system considered in this paper is able to transmit real valued baseband signals only. Thus, the OFDM signal has to be generated in a special manner to ensure that this requirement is fulfilled, e.g. by complex conjugate extension of the subcarriers. For the theoretical considerations made in this work, the OFDM signal is modelled by a real valued process $X(t)$ with a gaussian probability density function

$$p_X(x) = \frac{1}{\sqrt{2\pi\sigma_X^2}} e^{-\frac{x^2}{2\sigma_X^2}}, \quad (1)$$

where σ_X^2 is the variance of the gaussian process. This signal $x(t)$ – being a realization of the process $X(t)$ – is fed into a chain of nonlinearities

$$z(t) = \beta^2 \cos^2(m \cdot c(x(t)) + u_{\text{bias}}), \quad (2)$$

where $c(\cdot)$ represents a hard clipping characteristic with lower and upper clipping thresholds c_{low} and c_{high} , see figure 1. The cosine characteristic

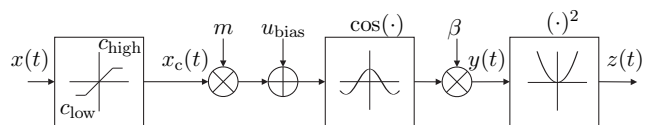


Fig. 1. Schematic representation of the nonlinear system

is caused by the Mach-Zehnder modulator (MZM) used for intensity modulation of the laser light source [1]. The squaring operation takes place at the receiver, where the instantaneous light power is detected by a photo diode. m and u_{bias} are user controllable system parameters that control drive level and operation point of the modulator (therefore m is restricted to positive values), β is a positive

gain factor used for controlling the optical power on the channel. The clipping operation is required to avoid driving the modulator over the reversal points of the cosine-square characteristic curve in order to stay in the monotonically increasing region $[-\pi/2, 0]$ and thus are dependent on m and u_{bias} . In practical applications, the clipping device would be placed behind the addition of u_{bias} , directly in front of the MZM, to allow fixed clipping thresholds $\vartheta_{\text{low}} = -\pi/2$, $\vartheta_{\text{high}} = 0$. However, these models are mathematically equivalent and can be translated into each other by use of the relations

$$\begin{aligned} \vartheta_{\text{low}} &= mc_{\text{low}} + u_{\text{bias}} \\ \vartheta_{\text{high}} &= mc_{\text{high}} + u_{\text{bias}}. \end{aligned} \quad (3)$$

However, the model in (2) is preferred due to its more pleasing mathematical representation, which will be used in the following section.

III. STOCHASTICAL MEASURES OF THE RECEIVER OUTPUT SIGNAL

The receiver output signal $z(t)$ is a realization of a stochastic process $Z(t)$, which can be decomposed into a scaled version of the originally transmitted signal (corresponding to an SNR loss) and an uncorrelated distortion term $D(t)$ [2],[3]:

$$Z(t) = \alpha X(t) + D(t). \quad (4)$$

The scaling factor α will be calculated in the following using these variables, as will be the second order moment of $Z(t)$. Hence, the power of the interference term $D(t)$ can be evaluated.

For calculation of α , the fact that $D(t)$ is uncorrelated to $X(t)$ can be employed. For the cross correlation of $X(t)$ and $Z(t)$, we find:

$$\begin{aligned} r_{XZ}(\tau) &= \text{E} \{X(t)Z(t + \tau)\} \\ &= \alpha \text{E} \{X(t)X(t + \tau)\} = \alpha r_{XX}(\tau) \end{aligned} \quad (5)$$

Evaluating this equation at $\tau = 0$, we obtain the relationship

$$\alpha = \frac{r_{XZ}(0)}{r_{XX}(0)} = \frac{r_{XZ}(0)}{\sigma_X^2}. \quad (6)$$

$r_{XZ}(0)$ can be calculated analytically:

$$\begin{aligned} r_{XZ}(0) &= \text{E} \{X(t)Z(t)\} \\ &= \int_{-\infty}^{\infty} x(t) \beta^2 \cos^2(m \cdot c(x(t)) + u_{\text{bias}}) p_X(x) dx. \end{aligned} \quad (7)$$

Using the piecewise definition of the overall nonlinearity

$$z(t) = \begin{cases} \beta^2 \cos^2(m \cdot c_{\text{low}} + u_{\text{bias}}) & x(t) \leq c_{\text{low}} \\ \beta^2 \cos^2(m \cdot x(t) + u_{\text{bias}}) & c_{\text{low}} < x(t) < c_{\text{high}} \\ \beta^2 \cos^2(m \cdot c_{\text{high}} + u_{\text{bias}}) & c_{\text{high}} \leq x(t) \end{cases}, \quad (8)$$

the integral in (7) can be split into three integrals:

$$\begin{aligned} r_{XZ}(0) &= \beta^2 \cos^2(m \cdot c_{\text{low}} + u_{\text{bias}}) \int_{-\infty}^{c_{\text{low}}} x(t) p_X(x) dx \\ &+ \int_{c_{\text{low}}}^{c_{\text{high}}} x(t) \beta^2 \cos^2(m \cdot x(t) + u_{\text{bias}}) p_X(x) dx \\ &+ \beta^2 \cos^2(m \cdot c_{\text{high}} + u_{\text{bias}}) \int_{c_{\text{high}}}^{\infty} x(t) p_X(x) dx. \end{aligned} \quad (9)$$

After evaluation and simplification, we get

$$\begin{aligned} r_{XZ}(0) &= \frac{\beta^2 m}{2} \sigma_X^2 e^{-2m^2 \sigma_X^2} \\ &\cdot \text{Im} \left\{ e^{-j2u_{\text{bias}}} \left(\text{erf}\left(\frac{c_{\text{low}}}{\sqrt{2\sigma_X^2}} + jm\sqrt{2\sigma_X^2}\right) \right. \right. \\ &\quad \left. \left. - \text{erf}\left(\frac{c_{\text{high}}}{\sqrt{2\sigma_X^2}} + jm\sqrt{2\sigma_X^2}\right) \right) \right\}, \end{aligned} \quad (10)$$

where $\text{Im} \{ \cdot \}$ stands for the imaginary part of the enclosed expression. Note that here the complex error function $\text{erf}(\cdot)$ (as e.g. defined in [5]) is employed. The scaling factor α is obtained by division of (10) by σ_X^2 . The overall power at the detector output can be calculated by means of the second order moment of $Z(t)$:

$$\text{E} \left\{ |Z(t)|^2 \right\} = \int_{-\infty}^{\infty} \beta^4 \cos^4(m \cdot c(x(t)) + u_{\text{bias}}) p_X(x) dx. \quad (11)$$

Using a similar approach as above, we find

$$\begin{aligned} \text{E} \left\{ |Z(t)|^2 \right\} &= \frac{1}{2} \left(1 + \text{erf}\left(\frac{c_{\text{low}}}{\sqrt{2\sigma_X^2}}\right) \right) \\ &\quad \cdot \beta^4 \cos^4(m \cdot c_{\text{low}} + u_{\text{bias}}) \\ &+ \int_{c_{\text{low}}}^{c_{\text{high}}} \beta^4 \cos^4(m \cdot x(t) + u_{\text{bias}}) p_X(x) dx \end{aligned}$$

$$+ \frac{1}{2} \left(1 - \operatorname{erf} \left(\frac{c_{\text{high}}}{\sqrt{2}\sigma_X} \right) \right) \cdot \beta^4 \cos^4(m \cdot c_{\text{high}} + u_{\text{bias}}), \quad (12)$$

which results in (13), where $\mathbf{Re}\{\cdot\}$ stands for the real part of the enclosed expression. Since the power of the desired (zero-mean) signal can easily be given as $\alpha^2\sigma_X^2$,

$$\mathbb{E} \left\{ |D(t)|^2 \right\} = \mathbb{E} \left\{ |Z(t)|^2 \right\} - \alpha^2\sigma_X^2 \quad (14)$$

is the power of the uncorrelated, non zero-mean distortion term. The mean $\mathbb{E}\{D(t)\}$ of the distortion term is equal to the mean of the process $\mathbb{E}\{Z(t)\}$, since $X(t)$ was assumed to be zero-mean. The moment $\mathbb{E}\{Z(t)\}$ can be calculated using the same approach as above in (12), resulting in (15). Since the OFDM subcarrier at baseband frequency 0 often is left unused for data transmission due to issues arising from DC offset problems, the power contained in this offset $\mathbb{E}\{D(t)\}$ does not contribute to the distortion of the OFDM signal. Thus it has to be subtracted for the following considerations.

IV. SIMULATION RESULTS

Figure 2 shows the Signal-to-Interference power ratio (SIR) $\alpha^2/(\mathbb{E}\{|D|^2\} - \mathbb{E}\{Z\}^2)$ for a normalized drive level $m \cdot \sigma_X$ in the range $[0, \frac{\pi}{2}]$ and an offset $-\frac{\pi}{2} \leq u_{\text{bias}} \leq 0$. The maximum SIR is obtained for $u_{\text{bias}} = -\frac{\pi}{4}$ and m tending towards 0. This behaviour is expected, since $u_{\text{bias}} = -\frac{\pi}{4}$ sets up the operation point in the point of maximum linearity

of the cosine-square characteristic. Furthermore, the smaller the driving level, the lesser the modulator is driven out of the operation point.

The SIR performance shown above determines

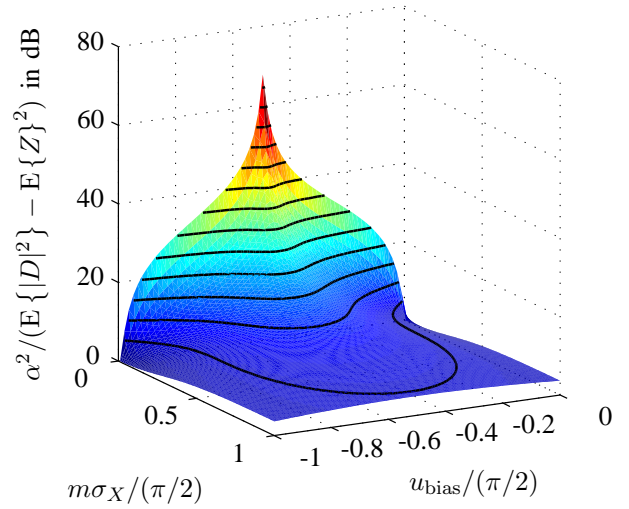


Fig. 2. Signal-to-Interference power ratio (logarithmic scale) for different values of $m\sigma_X$ and u_{bias}

the error-floor behaviour of a transmission system, as is shown in fig. 3 for a 32 subcarrier QPSK transmission system without guard interval in the back-to-back case with only additive white gaussian noise (AWGN) of overall power P_n (in the used bandwidth) being present.

A. Power constraints on the optical channel

Similarly to wireless communications, also in fiber optic communication systems power constraints

$$\begin{aligned} \mathbb{E} \left\{ |Z(t)|^2 \right\} &= \frac{\beta^4}{2} \cos^4(m c_{\text{low}} + u_{\text{bias}}) \left(1 + \operatorname{erf} \left(\frac{c_{\text{low}}}{\sqrt{2}\sigma_X} \right) \right) + \frac{\beta^4}{2} \cos^4(m c_{\text{high}} + u_{\text{bias}}) \cdot \left(1 - \operatorname{erf} \left(\frac{c_{\text{high}}}{\sqrt{2}\sigma_X} \right) \right) \\ &\quad - \frac{\beta^4}{16} e^{-8m^2\sigma_X^2} \mathbf{Re} \left\{ e^{-4ju_{\text{bias}}} \cdot \left(\operatorname{erf} \left(\frac{c_{\text{low}}}{\sqrt{2}\sigma_X} + 2jm\sqrt{2}\sigma_X \right) - \operatorname{erf} \left(\frac{c_{\text{high}}}{\sqrt{2}\sigma_X} + 2jm\sqrt{2}\sigma_X \right) \right) \right\} \\ &\quad - \frac{\beta^4}{4} e^{-2m^2\sigma_X^2} \mathbf{Re} \left\{ e^{-2ju_{\text{bias}}} \cdot \left(\operatorname{erf} \left(\frac{c_{\text{low}}}{\sqrt{2}\sigma_X} + jm\sqrt{2}\sigma_X \right) - \operatorname{erf} \left(\frac{c_{\text{high}}}{\sqrt{2}\sigma_X} + jm\sqrt{2}\sigma_X \right) \right) \right\} \\ &\quad - \beta^4 \frac{3}{16} \left(\operatorname{erf} \left(\frac{c_{\text{low}}}{\sqrt{2}\sigma_X} \right) + \operatorname{erf} \left(\frac{c_{\text{high}}}{\sqrt{2}\sigma_X} \right) \right) \end{aligned} \quad (13)$$

$$\begin{aligned} \mathbb{E} \{ Z(t) \} &= \beta^2 \mathbb{E} \left\{ \cos^2(m c(X(t)) + u_{\text{bias}}) \right\} \\ &= \frac{\beta^2}{2} \cos^2(m c_{\text{low}} + u_{\text{bias}}) \cdot \left(1 + \operatorname{erf} \left(\frac{c_{\text{low}}}{\sqrt{2}\sigma_X} \right) \right) + \frac{\beta^2}{2} \cos^2(m c_{\text{high}} + u_{\text{bias}}) \cdot \left(1 - \operatorname{erf} \left(\frac{c_{\text{high}}}{\sqrt{2}\sigma_X} \right) \right) \\ &\quad + \frac{\beta^2}{4} e^{-2m^2\sigma_X^2} \mathbf{Re} \left\{ e^{-j2u} \left(\operatorname{erf} \left(\frac{c_{\text{high}}}{\sqrt{2}\sigma_X} + jm\sqrt{2}\sigma_X \right) - \operatorname{erf} \left(\frac{c_{\text{low}}}{\sqrt{2}\sigma_X} + jm\sqrt{2}\sigma_X \right) \right) \right\} \\ &\quad + \frac{\beta^2}{4} \left(\operatorname{erf} \left(\frac{c_{\text{high}}}{\sqrt{2}\sigma_X} \right) - \operatorname{erf} \left(\frac{c_{\text{low}}}{\sqrt{2}\sigma_X} \right) \right) \end{aligned} \quad (15)$$

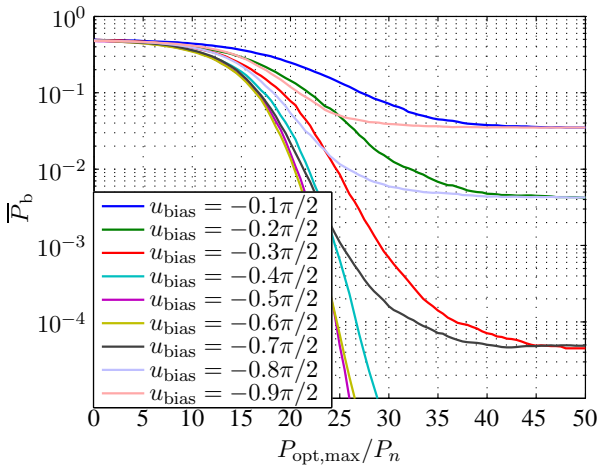


Fig. 3. BER performance for different values of u_{bias} and $m\sigma_X = \frac{\pi}{8}$

apply. Whereas in wireless systems, the transmit power is limited due to regulatory reasons or e.g. battery life in mobile applications, the optical power has to be limited to avoid nonlinear effects in the fiber, which occur at transmit powers over approximately 1 mW [1].

The optical power at the output of the Mach-Zehnder modulator after scaling by β can be calculated by means of the second order moment of the scaled modulator output signal $Y(t)$ which has already been calculated in (15):

$$\begin{aligned} P_{\text{opt}} &= \text{E} \left\{ |Y(t)|^2 \right\} = \text{E} \left\{ Z(t) \right\} \\ &= \beta^2 \underbrace{\text{E} \left\{ \cos^2(mc(X(t)) + u_{\text{bias}}) \right\}}_{=: P_0}. \end{aligned} \quad (16)$$

In order to fulfill a power constraint $P_{\text{opt,max}}$ on the optical channel exactly, the value of β has to be chosen as

$$\beta = \sqrt{\frac{P_{\text{opt,max}}}{P_0}}. \quad (17)$$

Regarding bit error performance, using such a constraint will cause BER curves to be shifted by $20 \log_{10} \beta$ dB into negative direction. Figure 4 shows the value of β for different values of $m\sigma_X$ and u_{bias} . Moving towards $u_{\text{bias}} = -\pi/2$, the mean of $Y(t)$ and thus the optical carrier power is reduced, allowing for an increased signal power. Applying the power constraint by choice of β as in (17) for $P_{\text{opt,max}} = \sigma_X^2$, the Signal-to-Interference+Noise Ratio (SINR) was calculated for a noise power $P_n = 0.1P_{\text{opt,max}}$. It is displayed in figure 5. The SINR is maximum for $u_{\text{bias}} \approx -0.89\pi/2$ and $m\sigma_X \approx 0.29\pi/2$. In this case the corresponding clipping

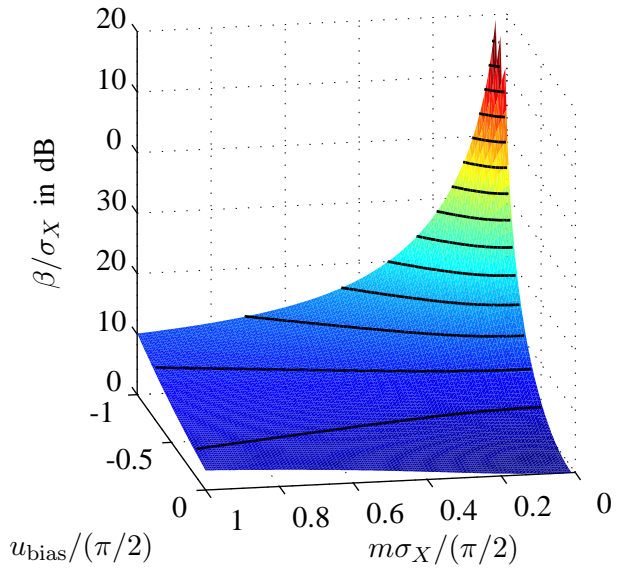


Fig. 4. Normalized scaling factor β for different values of $m\sigma_X$ and u_{bias}

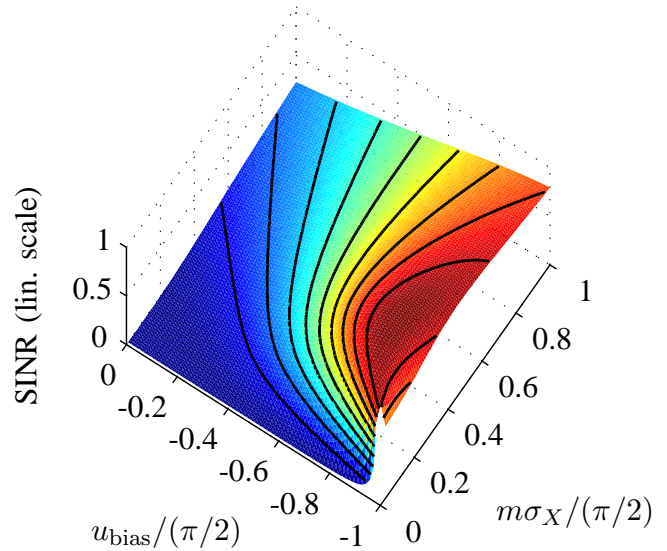


Fig. 5. SINR for a noise power $P_n = 0.1P_{\text{opt,max}}$ and varying values of $m\sigma_X$ and u_{bias}

thresholds are

$$\begin{aligned} c_{\text{low}} &= \frac{\pi}{2m} \left(-1 - \frac{u_{\text{bias}}}{\pi/2} \right) \approx -0.38\sigma_X \\ c_{\text{high}} &= -\frac{u_{\text{bias}}}{m} \approx 3.07\sigma_X, \end{aligned} \quad (18)$$

which means that in this operation point, almost half of the amplitude distribution is clipped, but the SINR improvement by an increase of β compensates for the higher power of the distortion terms. Figure 6 shows the bit error performance for the normalized drive level $m\sigma_X = 0.29\pi/2$ and different values of u_{bias} . The bit error curves for an SNR of $P_{\text{opt,max}}/P_n = 10$ dB – corresponding to

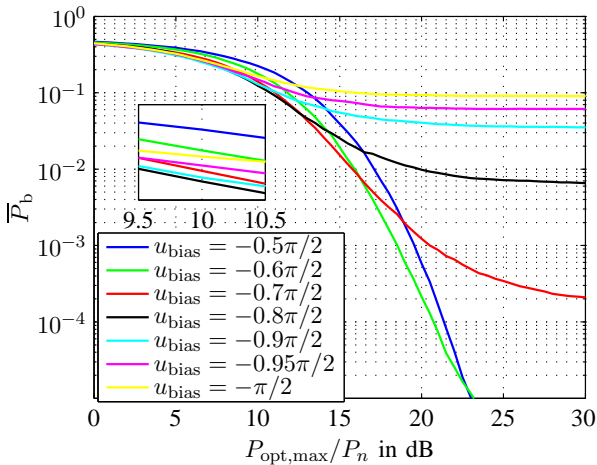


Fig. 6. BER performance for different values of u_{bias} and $m\sigma_X = 0.29\frac{\pi}{2}$

the scenario employed in the previous figure – is magnified in the subplot. While an offset $u_{\text{bias}} = -0.9\frac{\pi}{2}$ should show best performance according to the previous figure, here it is the case for $u_{\text{bias}} = -0.8\frac{\pi}{2}$. The SNR region in which the former value shows better performance is observed to lie below 10 dB. One explanation to this behaviour is that the interference introduced by nonlinear distortions does not necessarily follow a Gaussian distribution and – even more important – has a power spectral density that partially falls outside the OFDM band and influences different OFDM subcarriers in a different way. Analysis of the spectral properties of the interference is not subject of this work, but will be done in future publications.

B. Influence of Clipping Thresholds

Given a fixed drive level m and offset level u_{bias} , the question of dependence of the system performance on the clipping thresholds arises. From a naive point of view, moving the clipping thresholds away from the reversal points of the cosine-square characteristic towards the operation point might improve the system performance, since the deviation from a linear characteristic is strongest around the reversal points. On the other hand, the signal distortions introduced by clipping are increased. For this reason, the BER performance for clipping thresholds $\{\vartheta_{\text{low}}, \vartheta_{\text{high}}\} = \{-1, 0\} \frac{\pi}{2}, \{-0.9, -0.1\} \frac{\pi}{2} \dots \{-0.6, -0.4\} \frac{\pi}{2}$ has been simulated for an offset $u_{\text{bias}} = -0.5\frac{\pi}{2}$, i.e. in the linear operation point and a normalized drive level $m\sigma_X = 0.3\frac{\pi}{2}$, which in a power constrained scenario shows best performance for a target BER of 10^{-3} . Figure 7 shows that clipping thresholds

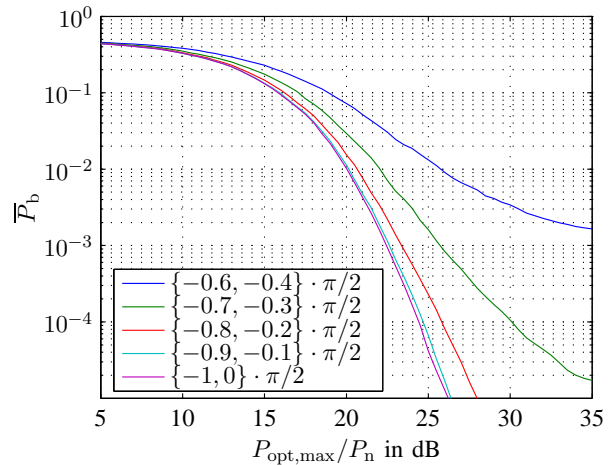


Fig. 7. BER performance for different clipping thresholds for $u_{\text{bias}} = -0.5\frac{\pi}{2}$ and $m\sigma_X = 0.3\frac{\pi}{2}$

$\{-0.9, -0.1\} \frac{\pi}{2}$ cause almost the same performance as clipping in $\{-1, 0\} \frac{\pi}{2}$. Using a smaller interval increases distortions which degrade the BER performance significantly.

V. CONCLUSIONS

First, a stochastic model for the nonlinearities present in transmitter and receiver components has been presented, then the error floor behaviour of the BER has been predicted on the basis of closed form expressions for expected Signal-to-Interference power ratios and verified using Monte-Carlo simulations. The results in [6] presented by our cooperation partner support the observations made in our investigations.

In future work, the considerations made in this paper will be transferred to complex valued systems as required for e.g. Single Sideband (SSB) transmission.

REFERENCES

- [1] G.P. Agrawal, *Fiber-Optic Communication Systems, Third Edition*, John Wiley & Sons, Inc., 2002.
- [2] J.J. Busgang, *Crosscorrelation Functions of Amplitude-Distorted Gaussian Signals*, PhD thesis, Massachusetts Institute of Technology, 1952.
- [3] P. Zillmann, *Empfangsalgorithmen für nichtlinear verzerrte Mehrträgersignale*, PhD thesis, Technical University of Dresden, 2007.
- [4] A.J. Lowery, Liang Du, J. Armstrong, *Orthogonal Frequency Division Multiplexing for Adaptive Dispersion Compensation in Long Haul WDM Systems*, Optical Fiber Communication Conference (OFC), PDP39, March 2006.
- [5] M. Abramowitz, I.A. Stegun, *Handbook of Mathematical Functions* New York: Dover Publications, Inc., 1968.
- [6] A. Ali, J. Leibrich, W. Rosenkranz, *Spectrally Efficient OFDM-Transmission over Single-Mode Fiber Using Direct Detection*, Proc. of the 13th International OFDM-Workshop (InOWo'08), August 27th/28th, Hamburg, Germany.